IEEE Photonics Journal
An IEEE Photonics Society Publication

Open Access

Investigation of Efficiency and Droop Behavior Comparison for InGaN/GaN Super Wide-Well Light Emitting Diodes Grown on Different Substrates

Volume 6, Number 6, December 2014

Tongbo Wei
Lian Zhang
Xiaoli Ji
Junxi Wang
Ziqiang Huo
Baojun Sun
Qiang Hu
Xuecheng Wei
Ruifei Duan
Lixia Zhao
Yiping Zeng
Jinmin Li

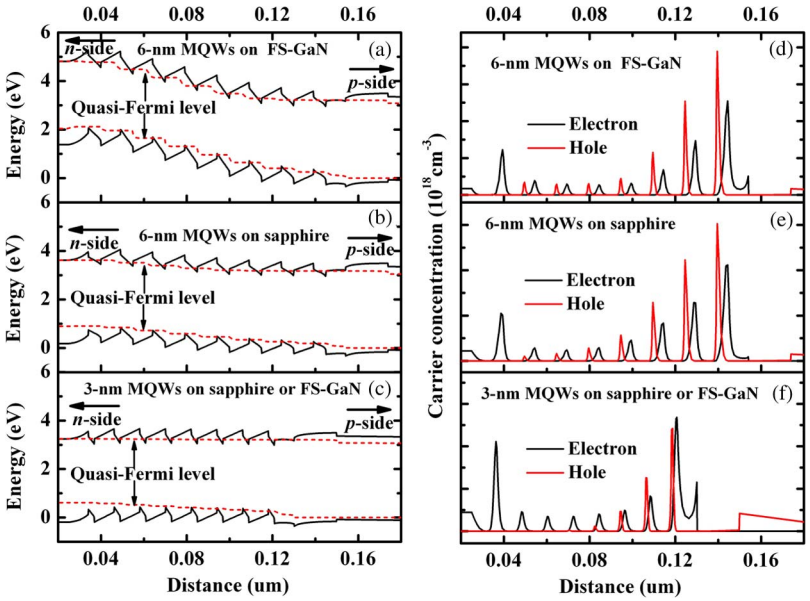

DOI: 10.1109/JPHOT.2014.2363428
1943-0655

Investigation of Efficiency and Droop Behavior Comparison for InGaN/GaN Super Wide-Well Light Emitting Diodes Grown on Different Substrates

Tongbo Wei,[1] Lian Zhang,[1] Xiaoli Ji,[1] Junxi Wang,[1] Ziqiang Huo,[1] Baojun Sun,[1] Qiang Hu,[1] Xuecheng Wei,[1] Ruifei Duan,[1] Lixia Zhao,[1] Yiping Zeng,[2] and Jinmin Li[1]

[1]State Key Laboratory of Solid-State Lighting, Institute of Semiconductors, Chinese Academy of Sciences, Beijing 100083, China
[2]Key Laboratory of Semiconductor Material Sciences, Institute of Semiconductors, Chinese Academy of Sciences, Beijing 100083, China

DOI: 10.1109/JPHOT.2014.2363428

Manuscript received September 2, 2014; revised October 2, 2014; accepted October 4, 2014. Date of current version October 29, 2014. This work was supported by the National Natural Sciences Foundation of China under Grant 61274040 and Grant 61474109, the National Basic Research Program of China under Grant 2011CB301902, the National High Technology Program of China under Grant 2014AA032605, and the Youth Innovation Promotion Association, Chinese Academy of Sciences. Corresponding author: T. Wei (e-mail: tbwei@semi.ac.cn).

Abstract: In this work, efficiency droop of InGaN/GaN multiple-quantum-well LEDs with super wide well (WW) is discussed by comparing the external quantum efficiency (EQE) of GaN grown on sapphire and FS-GaN substrates. The luminescence and electrical characteristics of these WW LEDs are also experimentally and theoretically analyzed. With the increase of well width from 3 nm to 6 nm, high V-pits density and more strain relaxation are found in WW LED on sapphire, which exhibits greatly reduced peak efficiency but almost negligible droop behavior. In contrast, despite a larger polarization field, WW LED on FS-GaN shows obviously enhanced peak efficiency and comparable droop compared to the counterpart with 3-nm well. The Auger recombination probably dominates the mechanism of efficiency droop rather than defect-related nonradiative recombination or polarization effect in the WW LED on both sapphire and FS-GaN, especially at high current density.

Index Terms: Light-emitting diodes, optical devices.

1. Introduction

III-nitride wide bandgap light-emitting diodes (LEDs) have recently attracted considerable interest due to their various applications, such as traffic signals, back-side lighting in liquid crystal displays, and illumination lighting by white light LEDs. However, the development of high-brightness InGaN LEDs suffers from severe efficiency reduction with increasing the current, known as the efficiency droop. To make LEDs suitable for application in high-power solid-state general lighting, it is imperative to recognize and overcome the efficiency droop phenomenon. At present, the fundamental mechanism that is responsible for the efficiency droop remains debatable, and various mechanisms regarding the droop origin such as carrier delocalization [1],

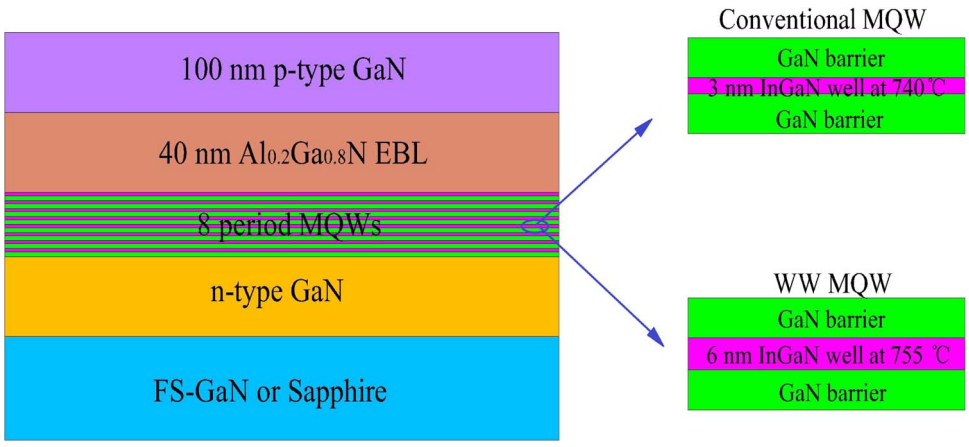

Fig. 1. Schematic diagram of InGaN based LED structures with conventional MQWs of 3-nm thickness and WW MQWs of 6-nm thickness on sapphire and FS-GaN substrate.

Auger recombination [2], [3], insufficient hole injection [4], [5], defect-related tunneling [6], [7], and carrier leakage from the active region [8]–[11] have been proposed. Among them, the carrier-density dependent mechanism has been believed as the important candidate for origin of efficiency droop [12]. Because the Auger-related recombination loss scales with the cubic power of the free-carrier density, it is proposed as primary mechanisms of droop phenomenon, especially at high current densities [13].

Consequently, the realization of LED structure with decreased carrier density in the active region will be a promising concept with improved high current saturation. In previous reports, the optimization of well width and number of quantum well has been widely studied to enhance the internal quantum efficiency (IQE) of LEDs [8], [14]. However, the width of well structure exceeding 4 nm usually results in the stronger polarization effect between well and barrier and deteriorates IQE of LED, especially for multiple quantum well (MQW) LEDs. Thus, the well width of LEDs is mostly confined below 3.5 nm. Recently, to further reduce the carrier density, the super wide-well (WW) InGaN-based double-heterostructure (DH) [15] and sole quantum well (SQW) [16] LED structures have been reported, demonstrating the improved droop behavior. Nevertheless, until recently, there is still very limited literature on how efficiency droop characteristics of super WW ($\geq$ 4 nm) MQWs LEDs evolve, while such a study would be important for both physical understanding and future practical applications. From SQW to MQWs, the polarization effect and carrier transport in WW structure are urgent to be investigated. In this study, the luminescence and electrical characteristics of super WW InGaN/GaN MQWs structures grown on FS GaN substrate and sapphire are experimentally and theoretically investigated. We also focus on discussing the influences of the strain-induced piezoelectric effect and dislocation density on electroluminescence (EL) properties and efficiency droop behavior of these thick MQWs.

2. Device Structure and Fabrication

The blue InGaN/GaN LEDs were grown on *c*-plane sapphire and FS-GaN substrate with a dislocation density of about 2×10^7 cm^{-2} by metal-organic chemical vapor deposition (MOCVD). For direct comparisons, an optimized 2 μm GaN buffer layer were firstly grown on sapphire substrate prior to the LED growth. As shown in Fig. 1, the original LED structures were composed of 3 μm thick n-GaN layer, eight period of InGaN/GaN MQWs with 10 nm thick barriers, 40 nm thick $Al_{0.2}Ga_{0.8}N$ electron-blocking layer (EBL) and a 100 nm thick *p*-GaN layer. Here, in the MQWs, the 3-nm-thick quantum wells were grown at 740 °C, whereas the 6-nm-thick WWs were grown at 755 °C to obtain the same emission wavelength of blue emission. Especially, considering the good thermal conduct of FS GaN substrate, the growth temperature of LED structures on FS was increased 2 °C compared with that on sapphire substrate. Finally, the

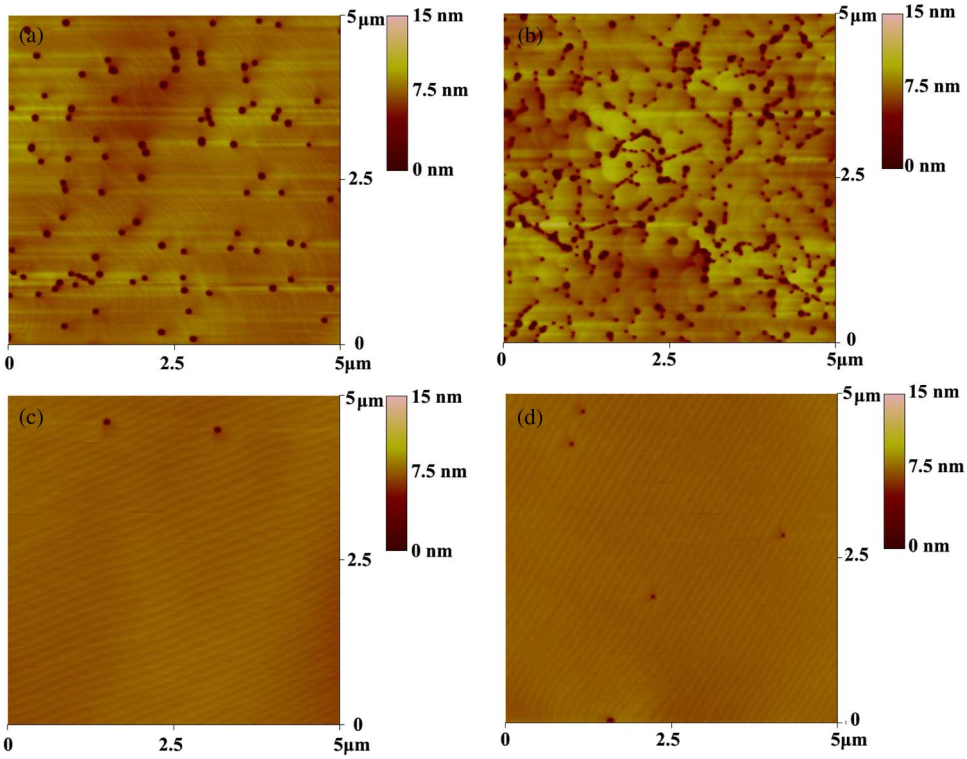

Fig. 2. AFM images $(5 \times 5\ \mu m^2)$ of the surface morphology of (a) 3-nm-thick and (b) 6-nm-thick MQWs on sapphire and (c) 3-nm-thick and (d) 6-nm-thick MQWs on FS-GaN substrate.

LEDs were fabricated with a conventional square mesa $(1 \times 1\ mm^2)$ using indium tin oxide (ITO) with a thickness of 200 nm as a transparent current spreading layer (TCL) and Cr/Pt/Au as the *n*- and *p*-electrodes by e-beam evaporation. To avoid the impact of light extraction, the backside of all the chips was polished and without the reflectivity mirror. The electrical and luminescence characteristics of the LEDs were measured at dc current with a calibrated integrating sphere. To prevent the self-heating effect when to measure the external quantum efficiency (η_{ext}) for droop, the devices were driven in pulsed mode with 1 KHz frequency and 0.1% duty cycle. The relaxation degree of InGaN/GaN MQWs and their indium compositions were studied by asymmetrical (105) X-ray reciprocal space mapping (RSM) with a Bede-D1 system.

3. Results

Surface morphology of InGaN/GaN MQWs with 3-nm-thick and 6-nm-thick wells grown on sapphire and FS-GaN substrates using tapping-mode atomic force microscopy (AFM) is shown in Fig. 2. Similar to the previous reports, many V-shaped defects appear on the surface of MQWs grown on sapphire, which are usually triggered by the treading dislocations and indium segregation [17], [18]. As shown in Figs. 1(b) and 2(a), 6-nm-thick MQWs on sapphire reveal larger pit density $(1.6 \times 10^9\ cm^{-2})$ than those with 3-nm-thick well $(3.7 \times 10^8\ cm^{-2})$. Besides, the size of pits in 6-nm-thick MQWs decreases due to enhanced surface diffusion of adatoms, following the well temperature increase of 15 °C. In contrast, the 3-nm-thick and 6-nm-thick MQWs grown on FS-GaN are comparable, almost without the surface pits, and the terrace-step structures are clearly seen, suggesting that smooth two-dimensional step-flow growth is achieved by homoepitaxial growth. The root-mean-square surface roughness increases from 1.43 nm to 1.92 nm for MQWs on sapphire, and instead decreases from 0.28 nm to 0.22 nm for those on FS-GaN, when the well width changes from 3 nm to 6 nm.

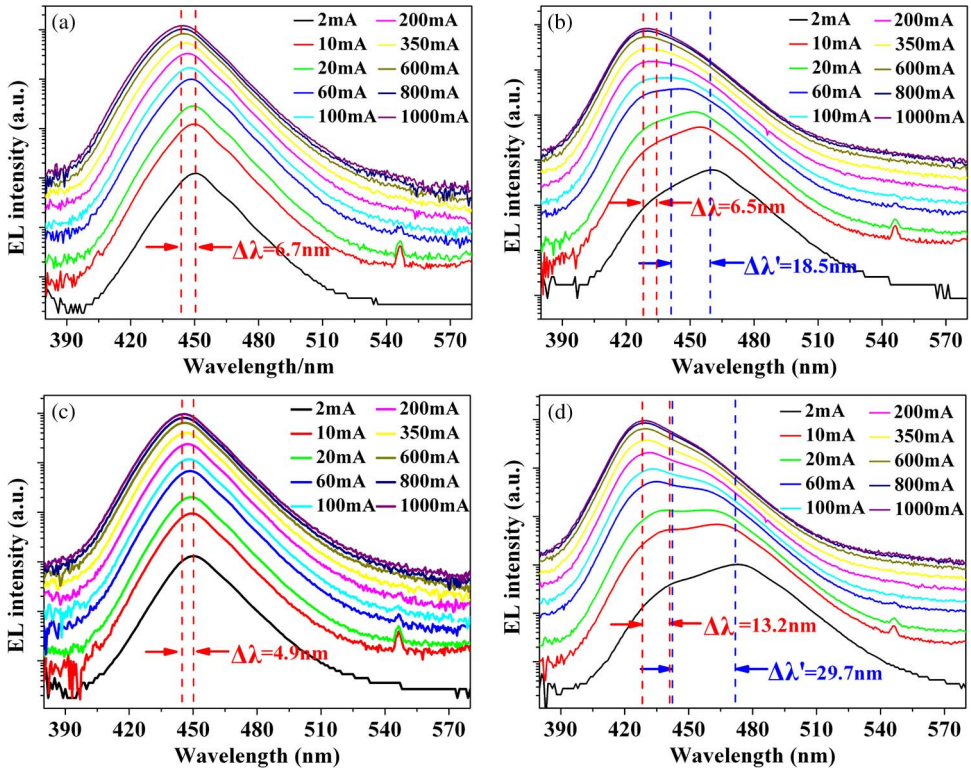

Fig. 3. Room-temperature EL spectra of LEDs with (a) 3-nm-thick and (b) 6-nm-thick MQWs on sapphire at various injection currents with peak wavelength shift indicated. (c) and (d) Corresponding well width LEDs on FS-GaN substrate.

Fig. 3 shows the room-temperature electroluminescence (EL) spectra of all LED samples under the pulsed injection currents with a 0.1% duty cycle. As the injected current increases from 2 mA to 1000 mA, the emission peak wavelength of 3-nm-thick MQW LED on FS-GaN substrate exhibits a blue-shift by 4.9 nm, which is less than 6.7 nm for that on sapphire. It is known that the extent of blueshift is strongly related to the strength of piezoelectric field in InGaN/GaN MQWs. Therefore, it is revealed there is weak internal polarization field in 3-nm-thick MQWs grown on FS-GaN compared on sapphire, due to relatively low strain in the homo-epitaxial layers. In contrast, the blueshifts $(\Delta\lambda)$ of 6-nm-thick MQWs grown FS-GaN and sapphire are 13.2 nm and 6.5 nm, respectively. It is expectable that a stronger polarization effect happens when a thicker well of InGaN is grown on GaN barrier, followed by the larger compressive strain. However, the anomalous behavior appears for 6-nm-thick MQWs on sapphire, even with a smaller blueshift than 3-nm-thick MQWs. The origination of weak polarization field in WW LED on sapphire will be discussed below. In addition, irrespective of the type of substrates, the 6-nm-thick WW LEDs show two distinguished emission peaks. In Fig. 3(b) and (d), the longer extra peak is dominated under the current up to 200 mA for WW LED on sapphire, while the longer emission is exceeded after 20 mA current for that on FS-GaN. Laubsch *et al.* [19] also found the two peaks in the 5 nm wide SQW LED and they attributed the origin of long and short emission to the ground-state and excited state recombinations, respectively. However, a large peak blueshift $(\Delta\lambda')$ of the longer emission is found as 18.5 nm and 29.7 nm for WW LEDs on sapphire and FS-GaN, respectively, as the current increases from 2 mA to 1000 mA. Even under the low current from 2 mA to 10 mA, the blueshift of longer emission also reaches 5.9 nm and 9.6 nm, respectively. Due to the low levels of injection current, band filling and charge screening effects of MQWs is negligible. Therefore, the long emission does not originate from the band-to-band ground-state recombination according to such a large shift. Furthermore, it is noted that the EL intensity of long emission shows a sublinear increase as the injection current increases,

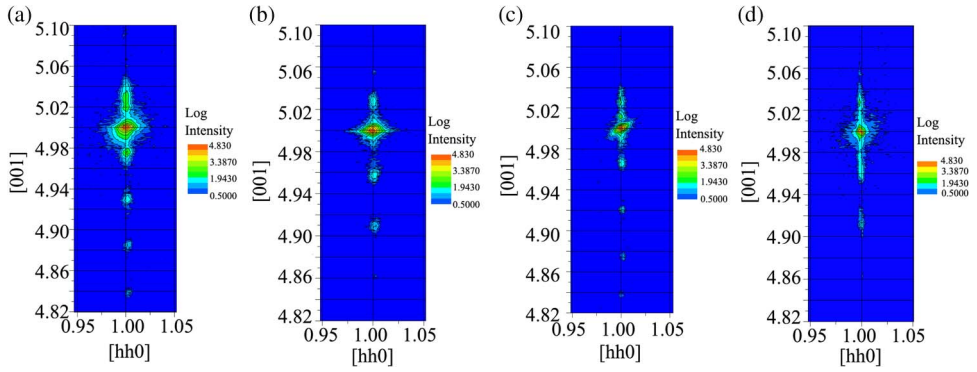

Fig. 4. X-ray RSM around the asymmetric (105) reflection for (a) 3-nm-thick and (b) 6-nm-thick MQWs on sapphire and (c) 3-nm-thick and (d) 6-nm-thick MQWs on FS-GaN substrate.

which is typical dependence for deep-level recombination [20]. Considering the facts that the two emission peaks are only observed in WW MQWs, we may conclude the long emission originates from the indium-rich dots in the thick InGaN alloy [21], [22]. Regardless of substrates, severe indium separation would occur due to the stronger polarization effect in the 6-nm thick MQWs, compared to that in 3-nm MQWs. The long emission in WW MQWs on GaN substrate obviously weakens than that on sapphire due to low compressive stress during the homoepitaxial growth, which also validates the assumption.

To further understand the anomalous EL spectra of WW LEDs, we perform the RSM to investigate the structural properties of these MQWs. Fig. 4 shows RSM around the asymmetric (105) reflection for 3-nm and 6-nm thick MQWs LEDs grown on sapphire and FS-GaN substrates. For the same well-width, the distance between GaN and zero-order satellite peak for the two samples are almost identical, meaning the same average indium composition. For 3-nm and 6-nm thick MQWs on GaN substrate, the main GaN peak and the zero-order diffraction satellite peak of the InGaN/GaN MQWs are aligned in a vertical line parallel to the Qy axis in Fig. 4(c) and (d), indicating almost fully-strain with no relaxation along the plane direction. However, due to the heteroepitaxial growth, there is a relaxation degree of about 9% in 3-nm MQWs LED on sapphire in Fig. 4(a). Furthermore, with the increase of well width, more strain relaxation occurs within the 6-nm thick MQWs on sapphire shown in Fig. 4(b), reaching 30% of relaxation degree. As the strain relaxation occurs within the InGaN MQWs, the misfit-induced defects such as threading dislocations or stacking faults are usually generated [23]. Here, the larger mismatch in 6-nm MQWs LED on sapphire results in the distinct strain relaxation, followed by the formation of high density of V-pits shown in Fig. 2(b). The V-pits number in AFM results indicates good relation with the stress relaxation obtained by RSM. In this case, more stress relaxation in WW on sapphire compensates the internal polarization field and, thus, cause a small peak blueshift in EL spectra at various currents.

Fig. 5(a) shows the semilogarithmic current-voltage (I–V) characteristics of all the LEDs. The I–V curves of these LEDs are shown to be almost identical at voltages higher than 2.5 V. However, the rise of forward current in WW LEDs occurs at a lower forward voltage (1.4 V) than that in 3-nm-thick MQW LEDs (1.7 V on sapphire and 1.9V on FS-GaN). The calculated diode ideality factors are 4.5 and 5.5 for WW LED on sapphire and on FS-GaN in the forward voltage range of 1.4 to 2.0 V, respectively. In contrast, ideality factor appears as large as 4.0 for 3-nm MQW LED on sapphire and 3.3 for that on FS-GaN in the range of 1.9 to 2.5 V. Here, the high value of ideality factors for WW LEDs at low bias means that the defect-assisted tunneling process rather than diffusion and recombination are responsible for the current conduction [24], originated due to high density of defects. The suppression of forward leakage current in 3-nm MQW LED on FS-GaN is the most pronounced, corresponding to the reduced defects in homo-epitaxial growth. For WW MQWs LEDs, there are indium separation and defects with high density, relating with high value of ideality factor. It is surprising that the WW LED on sapphire has a lower ideality

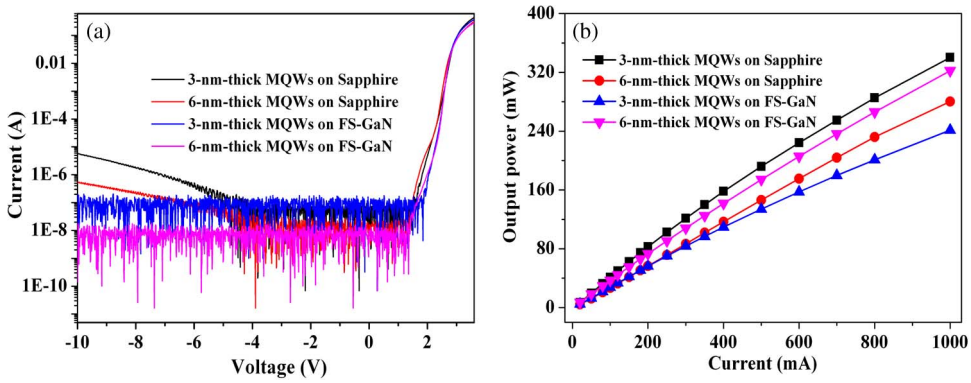

Fig. 5. (a) Semilogarithmic *I–V* characteristics of the LEDs with different well width on sapphire and FS-GaN. (b) Light output powers of the LEDs on sapphire and FS-GaN as the functions of injecting current.

factor than that on GaN substrate. Han *et al.* [25] reported LEDs with intentionally formed V-shaped pits showed a low diode ideality factor and attributed to the electrical passivation of dislocations due to the highly resistive region grown on semipolar V-shaped pits facets. Thus, we speculate that lots of V-pits on the surface WW MQWs on sapphire resemble the analogous effect of electrical passivation. Therefore, the leakage path is not absolutely determined by the V-pits amount and more details work need to be carried out. On the other hand, it is noted that WW structures don't deteriorate the reverse leakage of the LEDs. At a typical reverse-bias of -10 V, the leakage currents of 3-nm-thick MQW LEDs on sapphire and FS-GaN are 5.7×10^{-6} A and 6.3×10^{-8} A, respectively, while the leakage currents of WW LEDs on sapphire and FS-GaN are only 5.3×10^{-7} A and 8.1×10^{-9} A, respectively. The reverse leakage of InGaN/GaN LED has been attributed to the electron tunneling from p-GaN to n-GaN through dislocations or defects [26]. Homoepitaxial grown LEDs obviously suppress the electron tunneling due to the significantly reduced density of V-pits. Furthermore, the improvement of reverse tunneling current of WW LEDs is attributed to the increased energy barrier induced by the higher energy state of InGaN well layer on the semipolar facet of V-pits, compared to that with 3-nm MQWs. Usually, there is a strong correlation of reverse leakage current and forward turn-on voltage. However, the trend discrepancy of reverse and forward currents in WW LEDs will be needed in more experiments to clarify.

The optical output power of the LEDs on sapphire and FS-GaN as a function of the forward current with a duty cycle of 0.1% is shown in Fig. 5(b), without any methods used to improve light extraction. Based on the smooth backside, it is noted that the output power of 3-nm-thick MQWs LED on sapphire instead surpasses the counterpart grown on FS-GaN due to smaller refractive index and higher transparency of sapphire compared to bulk GaN. For the LEDs on sapphire, the output power with 6-nm-thick WW is decreased by 27.2% compared to that with 3-nm-thick MQW at 350 mA current. In contrast, 6-nm-thick WW LED on FS-GaN shows the improvement of 30.2% compared with the counterpart with 3-nm-thick MQW. Therefore, it is concluded that the optimal well width of LEDs may be increased with the decrease of the defect density in LEDs, which is consistent with the previous study of SQW LEDs [16].

Fig. 6 compares the external quantum efficiency (EQE) versus current for these LEDs. With the increase of well width from 3 nm to 6 nm, the LED on sapphire exhibits obviously reduced peak efficiency, but almost negligible droop behavior with a delayed onset of droop until 60 A/cm^2. The low peak efficiency is attributed to the fact that the nonradiative recombination is dominated due to high density V-pit defects in thick well LED on sapphire. At low current most of carriers may preferentially enter into V-defects and undergo nonradiative recombination. As the injected current increases, there will be more and more carriers entering into QWs to recombine radiatively since the leakage carriers into V-defects will go closer to saturation. For WW

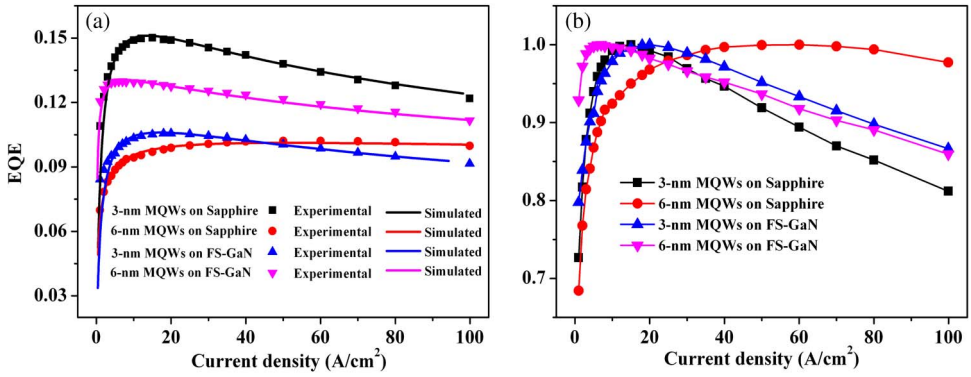

Fig. 6. (a) EQE of the LEDs (solid dot) and theoretical fit to the measured data (solid line) based on carrier's rate equation as a function of injection current. (b) Normalized EQE these LEDs.

LED on sapphire with very high density of V-shaped pits, obvious strain relaxation in WW MQWs occurs, weakening the internal polarization field. Therefore, the fact WW LED on sapphire has almost no droop may be attributed to its lowest carriers density in WW resulted from the weakest polarization effect and increased well width. In contrast, the thick well LED on FS-GaN shows greatly enhanced peak efficiency compared to 3-nm well LED. It is also noted that the peak efficiency current density of 6-nm well LED on FS-GaN is brought forward to 7 A/cm^2 in comparison with 20 A/cm^2 of 3-nm well LED, but the efficiency droop of the two LEDs is comparable, about 14% at 100 A/cm^2. The decrease of peak efficiency current for WW LED on FS-GaN is attributed to the strong polarization effect, and not the V-defects, combined with the XRD RSM results. Until high current, the advantage of WW structure with low carrier density is realized as almost same droop in comparison with the LED with 3-nm well. On the other hand, the WW LED on FS-GaN does't suffer from the serious nonradiative recombination caused by V-pits defects. The high polarization effect in WW does't deteriorate the LED EL intentisy. The higher peak efficiency of WW LED on FS-GaN is attributed to the sufficient carrier confinement in the active region due to the small quantization energies in the wide well, compared to that 3-nm well LED [16]. Unlike the LEDs on sapphire, WW structure on FS-GaN achieves the mutual benefit of both high efficiency and low droop, as a promising approach to obtain high efficiency for homoepitaxial LEDs.

For the exploration of physical origin of efficiency droop in WW LEDs, we perform the simulation of afore-mentioned LEDs structure using the APSYS simulation software. Commonly accepted parameters are used in the simulations as listed in Ref. [27]. Fig. 7(a)–(c) show the calculated energy band diagrams of the MQWs with 3 and 6 nm width at a forward current of 15 A/cm^2. For 6-nm WW LED on FS-GaN, as a result of the polarization charges, a very severe situation of band bending, i.e., sloped triangular barriers and wells, is observed. In comparison, the band diagram of WW LED on sapphire is more uniform due to reduced polarization effect, followed by the formation of high density V-pits and revealed by XRD RSM. Fig. 7(d)–(f) show the carrier distribution in the whole InGaN/GaN MQWs structure at 15 A/cm^2 for the above LEDs. It is clear that both electrons and holes distributions in the WW LEDs become more uniform among the quantum well than those in 3-nm MQW LEDs, especially for holes. However, the quantum-confined stark effect (QCSE) in strained wells will deteriorate as the well width is increased. Large polarization field usually leads to the carrier overflow even at low current [28]. Thus, the WW LED on FS-GaN shows the low droop-onset current density (7 A/cm^2), corresponding to the strong QCSE. Further analysis is still needed to understand the essential mechanism, but the strong polarization effect plays a minor role in the trade-off of the original design goal, i.e., the suppression of Auger losses in WW LED on FS-GaN, especially higher current. This is attributed to the fact that as the current density increases, the

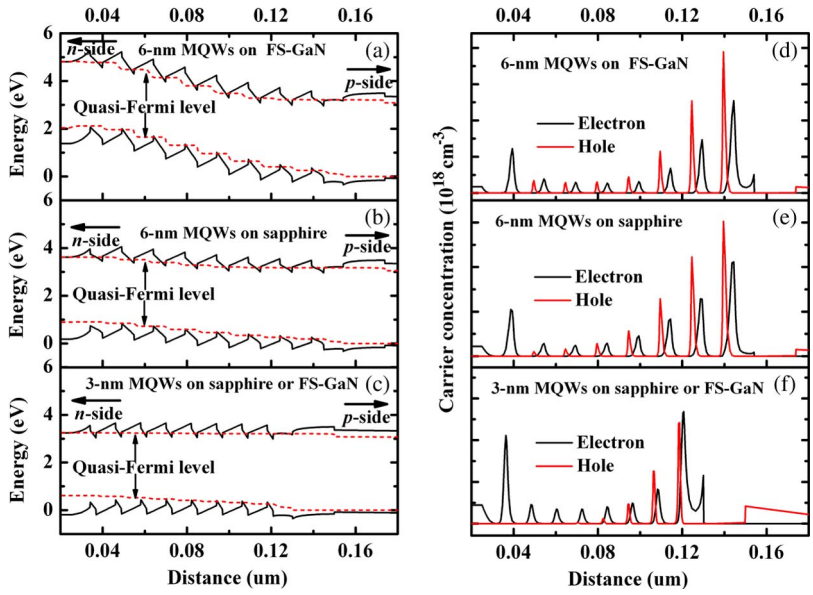

Fig. 7. (a)–(c) Calculated band diagram and (d)–(f) distribution of carrier concentration for 3-nm and 6-nm MQWs structures at 15 A/cm^2. The simulation of 3-nm MQWs on sapphire and FS is incorporated due to the same strain status according XRD mapping.

injected carriers will reduce the piezoelectric field due to increased screening electric field. This is the reason why the 6-nm and 3-nm MQW LEDs on FS-GaN have the similar droop rate despite the different peak efficiency current.

Finally, the influence of carrier density and Auger loss on the efficiency droop of WW LEDs is analyzed based on the rate equation. Assuming 100% injection efficiency and given the fact the leakage current can be ignored, the EQE can be expressed by a simple ABC model [29]–[32]

$$EQE = \eta_{extraction} \times IQE = \eta_{extraction} \times \frac{Bn^2}{An + Bn^2 + Cn^3} \tag{1}$$

where n represents the carrier concentration, and carrier recombination processes in MQWs mainly include Shockley-Read-Hall (SRH) nonradiative combination An, radiative recombination Bn^2, and Auger recombination Cn^3. According to (1), the efficiency droop is related to the Cn^3 term which dominates the total recombination rate at high current density. The value of C has been iteratively obtained by fitting the quantum efficiency as a function of the generation rate of carriers, as shown in Fig. 6(a). The C coefficient value of 3-nm and 6-nm MQW LEDs on sapphire is 1.2×10^{-29} cm^6 S^{-1} and 1.5×10^{-30} cm^6 S^{-1}, respectively, while the C value is 5.9×10^{-30} cm^6 S^{-1} and 3.3×10^{-30} cm^6 S^{-1} for 3-nm and 6-nm MQW LEDs on FS-GaN, respectively, which agree well with the reported values based on the optical pumping experiments [33]. It is noted that regardless the V-pits density, WW structures lead to the low C coefficient, which means weak Auger non-radiative recombination and droop behavior at high carrier density. This shows good agreement between the experiment data and our simulations. Cao *et al.* [34] also compared the characteristics of blue LEDs on sapphire and FS-GaN and argued dislocations were not responsible for the decrease in EQE of InGaN LEDs at elevated currents. Here, the WW LEDs on sapphire and FS-GaN also demonstrate that the dislocations play a minor role in droop behavior of LED, but exhibiting a large influence on EQE. Furthermore, combining the high EQE and low droop, more optimum WW width on FS-GaN and theoretical analysis are still needed to further clarify this issue.

4. Conclusion

In summary, we have investigated the efficiency droop phenomenon in super WW InGaN/GaN MQW LEDs grown on sapphire and FS-GaN. By using APSYS simulation, we detailedly discuss the influences of the dislocation density and strain-induced piezoelectric effect on EL properties and efficiency droop behavior of these WW LEDs. When compared with the conventional 3-nm MQW LED, WW LED on FS-GaN shows greatly enhanced peak efficiency and comparable droop, while the WW LED on sapphire exhibits reduced peak efficiency and negligible droop behavior. Furthermore, WW structure on FS-GaN achieves the mutual benefit of both high efficiency and low droop. This is a promising approach to obtain high efficiency for future homoepitaxial LEDs.

References

[1] B. Monemar and B. E. Sernelius, "Defect related issues in the 'current roll-off' in InGaN based light emitting diodes," *Appl. Phys. Lett.*, vol. 91, no. 18, pp. 181103-1–181103-3, Oct. 2007.

[2] E. Kioupakis, P. Rinke, K. T. Delaney, and C. G. Van de Walle, "Indirect Auger recombination as a cause of efficiency droop in nitride light-emitting diodes," *Appl. Phys. Lett.*, vol. 98, no.16, pp. 161107-1–161107-3, Apr. 2011.

[3] B. Galler *et al.*, "Experimental determination of the dominant type of Auger recombination in InGaN quantum wells," *Appl. Phys. Exp.*, vol. 6, no. 11, pp. 112101-1–112101-4, Oct. 2013.

[4] C. H. Wang *et al.*, "Hole injection and efficiency droop improvement in InGaN/GaN light-emitting diodes by band-engineered electron blocking layer," *Appl. Phys. Lett.*, vol. 97, no. 26, pp. 261103-1–261103-3, Dec. 2010.

[5] H.-Y. Ryu and J.-M. Lee, "Effects of two-step Mg doping in p-GaN on efficiency characteristics of InGaN blue light-emitting diodes without AlGaN electron-blocking layers," *Appl. Phys. Lett.*, vol. 102, no. 18, pp. 181115-1–181115-4, May 2013.

[6] N. I. Bochkareva *et al.*, "Defect-related tunneling mechanism of efficiency droop III-nitride light-emitting diodes," *Appl. Phys. Lett.*, vol. 96, no. 13, pp. 133502-1–133502-3, Mar. 2010.

[7] K. Akita, T. Kyono, Y. Yoshizumi, H. Kitabayashi, and K. Katayama, "Improvements of external quantum efficiency of InGaN-based blue light-emitting diodes at high current density using GaN substrates," *J. Appl. Phys.*, vol. 101, no. 33, pp. 033104-1–033104-5, Feb. 2007.

[8] Y.-L. Li, Y.-R. Huang, and Y.-H. Lai, "Efficiency droop behaviors of InGaN/GaN multiple-quantum-well light-emitting diodes with varying quantum well thickness," *Appl. Phys. Lett.*, vol. 91, no. 18, pp. 181113-1–181113-3, Oct. 2007.

[9] J. Lee *et al.*, "On carrier spillover in c- and m-plane InGaN light emitting diodes," *Appl. Phys. Lett.*, vol. 95, no. 20, pp. 201113-1–201113-3, Nov. 2009.

[10] B.-C. Lin *et al.*, "Hole injection and electron overflow improvement in InGaN/GaN light-emitting diodes by a tapered AlGaN electron blocking layer," *Opt. Exp.*, vol. 22, no. 1, pp. 463–469, Jan. 2014.

[11] D. S. Meyaard *et al.*, "Identifying the cause of the efficiency droop in GaInN light-emitting diodes by correlating the onset of high injection with the onset of the efficiency droop," *Appl. Phys. Lett.*, vol. 102, no. 25, pp. 251114-1–251114-4, Jun. 2013.

[12] A. Laubsch, M. Sabathil, J. Baur, M. Peter, and B. Hahn, "High-power and high-efficiency InGaN-based light emitters," *IEEE Trans. Electron Devices*, vol. 57, no. 1, pp. 79–87, Jan. 2010.

[13] R. Vaxenburg, E. Lifshitz, and A. L. Efros, "Suppression of Auger-stimulated efficiency droop in nitride-based light emitting diodes," *Appl. Phys. Lett.*, vol. 102, no. 3, pp. 031120-1–031120-5, Jan. 2013.

[14] S. C. Jain, M. Willander, J. Narayan, and O. R. Van, "III-nitrides: Growth, characterization, and properties," *J. Appl. Phys.*, vol. 87, no. 03, pp. 965–1006, Feb. 2000.

[15] N. F. Gardner *et al.*, "Blue-emitting InGaN-GaN double-heterostructure light-emitting diodes reaching maximum quantum efficiency above 200 A/cm^2," *Appl. Phys. Lett.*, vol. 91, no. 24, pp. 243506-1–243506-3, Dec. 2007.

[16] M. Maier, K. Köhler, M. Kunzer, W. Pletschen, and J. Wagner, "Reduced nonthermal rollover of wide-well GaInN light-emitting diodes," *Appl. Phys. Lett.*, vol. 94, no. 4, pp. 041103-1–041103-3, Jan. 2009.

[17] H. K. Cho, J. Y. Lee. G. M. Yang, and C. S. Kim, "Formation mechanism of V defects in the InGaN/GaN multiple quantum wells grown on GaN layers with low threading dislocation density," *Appl. Phys. Lett.*, vol. 79, no. 2, pp. 215–217, May 2001.

[18] K. Watanabe *et al.*, "Formation and structure of inverted hexagonal pyramid defects in multiple quantum wells InGaN/GaN," *Appl. Phys. Lett.*, vol. 82, no. 5, pp. 718–720, Dec. 2003.

[19] A. Laubsch *et al.*, "Luminescence properties of thick InGaN quantum-wells," *Phys. Status Solidi C*, vol. 6, no. S2, pp. S885–S888, Nov. 2009.

[20] A. Mao *et al.*, "Characteristics of dotlike green satellite emission in GaInN light emitting diodes," *Appl. Phys. Lett.*, vol. 98, no. 2, pp. 023503-1–023503-3, Jan. 2011

[21] G. Pozina *et al.*, "Origin of multiple peak photoluminescence in InGaN/GaN multiple quantum wells, *J. Appl. Phys.*, vol. 88, no. 5, pp. 2677–2681, Sep. 2000

[22] Y. Narukawa, Y. Kawakami, S. Fujita, S. Fujita, and S. Nakamura, "Recombination dynamics of localized excitons in In0.20Ga0.80N-In0.05Ga0.95 multiple quantum wells," *Phys. Rev. B*, vol. 55, no. 4, pp. R1938–R1941, Jan. 1997

[23] H. K. Cho, J. Y. Lee, and J. Y. Leem, "Strain relaxation behavior of the InGaN/GaN multiple quantum wells observed by transmission electron microscopy," *Appl. Surface Sci.*, vol. 221, no. 1–4, pp. 288–292, Jul. 2004.

[24] C. L. Reynolds, Jr. and A. Patel, "Tunneling entity in different injection regimes of InGaN light emitting diodes," *J. Appl. Phys.*, vol. 103, no. 8, pp. 086102-1–086102-3, Apr. 2008.
[25] S. H. Han *et al.* "Improvement of efficiency and electrical properties using intentionally formed V-shaped pits in InGaN/GaN multiple quantum well light-emitting diodes," *Appl. Phys. Lett.*, vol. 102, no. 25, pp. 251123-1–251123-4, Dec. 2013.
[26] Q. Shan *et al.*, "Transport-mechanism analysis of the reverse leakage current in GaInN light-emitting diodes," *Appl. Phys. Lett.*, vol. 99, no. 25, pp. 253506-1–253506-3, Dec. 2011.
[27] S.-C. Ling *et al.*, "Low efficiency droop in blue-green m-plane InGaN/GaN light emitting diodes," *Appl. Phys. Lett.*, vol. 96, no. 23, pp. 231101-1–231101-3, Jun. 2010.
[28] J. X. Wang, L. Wang, W. Zhao, Z. B. Hao, and Y. Luo, "Understanding efficiency droop effect in InGaN/GaN multiple-quantum-well blue light-emitting diodes with different degree of carrier localization," *Appl. Phys. Lett.*, vol. 97, no. 20, pp. 201112-1–201112-3, Nov. 2010.
[29] M. F. Schubert *et al.*, "Effect of dislocation density on efficiency droop in GaInN/GaN light-emitting diodes," *Appl. Phys. Lett.*, vol. 91, no. 23, pp. 231114-1–231114-3, Dec. 2007.
[30] Z. Q. Liu *et al.*, "Efficiency droop in InGaN/GaN multiple-quantum-well blue light-emitting diodes grown on free-standing GaN substrate," *Appl. Phys. Lett.*, vol. 99, no. 9, pp. 091104-1–091104-3, Aug. 2011.
[31] J.-Y. Chang *et al.*, "Numerical study of the suppressed efficiency droop in blue InGaN LEDs with polarization-matched configuration," *Opt. Lett.*, vol. 38, no. 16, pp. 3158–3161, Aug. 2013
[32] T. B. Wei *et al.*, "Efficiency improvement and droop behavior in nanospherical-lens lithographically patterned bottom and top photonic crystal InGaN/GaN light-emitting diodes," *Opt. Lett.*, vol. 39, no. 2, pp. 379–382, Jan. 2014
[33] Y. C. Shen *et al.*, "Auger recombination in InGaN measured by photoluminescence," *Appl. Phys. Lett.*, vol. 91, no. 14, pp. 141101-1–141101-3, Oct. 2007.
[34] X. A. Cao, Y. Yang, and H. Guo, "On the origin of efficiency roll-off in InGaN-based light-emitting diodes," *J. Appl. Phys.*, vol. 104, no. 09, pp. 093108-1–093108-4, Nov. 2008.